Since January 2020 Elsevier has created a COVID-19 resource centre with free information in English and Mandarin on the novel coronavirus COVID-19. The COVID-19 resource centre is hosted on Elsevier Connect, the company's public news and information website.

Indian Journal of Medical Microbiology 41 (2023) 45–52

Contents lists available at ScienceDirect

Indian Journal of Medical Microbiology

journal homepage: www.journals.elsevier.com/indian-journal-of-medical-microbiology

Original Research Article

An ultrastructural and genomic study on the SARS-CoV-2 variant B.1.210 circulating during the first wave of COVID-19 pandemic in India

Narendra Kumar [a], Rashmi Santhoshkumar [b], Pramada Prasad [a], Anson K. George [a], Jayashree Aiyar [c], Saurabh Joshi [c], Gayathri Narayanappa [b], Anita S. Desai [a], Vasanthapuram Ravi [a], Manjunatha M. Venkataswamy [a,*]

[a] Department of Neurovirology, National Institute of Mental Health and Neurosciences, Bengaluru, India
[b] Electron Microscopy -Common Research Facility, Department of Neuropathology, National Institute of Mental Health and Neurosciences, Bengaluru, India
[c] Discovery Biology, Syngene International Limited, Bengaluru, India

ARTICLE INFO

Keywords:
SARS-CoV-2
Genomic characterization
Phylogenetic analysis
Ultrastructure
India

ABSTRACT

Purpose: The study aims to isolate and understand cytopathogenesis, ultrastructure, genomic characteristics and phylogenetic analysis of SARS-CoV-2 virus of B.1.210 lineage, that circulated in India during first wave of the pandemic.

Methods: Clinical specimen from an interstate traveller from Maharashtra to Karnataka, in May 2020, who was positive by RT PCR for SARS-CoV-2 infection was subjected to virus isolation and Whole Genome Sequencing. Vero cells were used to study cytopathogenesis and ultrastructural features by Transmission Electron Microscopy (TEM). Phylogenetic analysis of the whole genome sequences of several SARS-CoV-2 variants downloaded from GISAID was performed in comparison with the B.1.210 variant identified in this study.

Results: The virus was isolated in Vero cells and identified by immunofluorescence assay and RT PCR. The growth kinetics in infected Vero cells revealed a peak viral titre at 24 h post-infection. Ultrastructural studies revealed distinct morphological changes with accumulation of membrane-bound vesicles containing pleomorphic virions in the cytoplasm, with single or multiple intranuclear filamentous inclusions and dilated rough endoplasmic reticulum with viral particles. Whole genome sequence of the clinical specimen as well as the isolated virus revealed the virus to be of lineage B.1.210 with the D614G mutation in the spike protein. Phylogenetic analysis of the whole genome sequence in comparison with other variants reported globally revealed that the isolated SARS-CoV-2 virus of lineage B.1.210 is closely related to the original Wuhan virus reference sequence.

Conclusions: The SARS-CoV-2 variant B.1.210 virus isolated here showed ultrastructural features and cytopathogenesis similar to that of the virus reported during early phase of pandemic. Phylogenetic analysis showed that the isolated virus is closely related to the original Wuhan virus, thereby suggesting that the SARS-CoV-2 lineage B.1.210 that was circulating in India during the early phase of pandemic is likely to have evolved from the original Wuhan strain.

1. Introduction

Coronaviruses (CoVs) are enveloped, single-stranded, positive-sense RNA viruses of the *Coronaviridae* family that cause respiratory illness among humans [1]. During the end of 2019, several cases of severe pneumonia caused by an unidentified virus were reported in the Wuhan city of Hubei province in China. Next-generation sequencing identified the causative agent as a novel coronavirus from the β coronavirus family [2]. The novel virus closely resembled the Severe Acute Respiratory Syndrome Coronavirus (SARS-CoV) and was named as SARS-COV-2 [3,4]. The disease caused by this novel virus was named Coronavirus disease 2019 (COVID-19) by World Health Organization [5]. COVID-19 was declared as a global pandemic on March 11, 2020 [6]. The first case in India was a medical student with travel history from Wuhan, China,

* Corresponding author.
E-mail address: manjuvswamy@gmail.com (M.M. Venkataswamy).

https://doi.org/10.1016/j.ijmmb.2022.12.009
Received 10 June 2022; Received in revised form 2 November 2022; Accepted 23 December 2022
Available online 6 January 2023

reported on January 30, 2020 [7]. Ever since, both symptomatic and asymptomatic cases have occurred in India, with a large proportion of cases (~90%) being asymptomatic [8].

During the first wave in India, strict lockdowns prevented the spread of the virus from high incidence states such as Maharashtra. However, a transient relaxation allowing people stranded in Maharashtra to travel to their respective states resulted in spread of the virus. Several genetic variants of SARS-CoV-2 have been reported from India [9,10]. The SARS-CoV-2 variant of lineage B.1.210 has been reported predominantly from Maharashtra along with a few other variants. Knowledge on the transmission dynamics and biological properties of new variants can guide targeted public health measures to reduce viral transmission. Further, the viral isolates can aid the development of newer vaccines and therapeutic agents [11].

The current study describes isolation, ultrastructural characterization, genomic sequencing and phylogenetic analysis of SARS-CoV-2 virus of B.1.210 lineage, that was circulating in India during the first wave of the pandemic, from an infected asymptomatic interstate traveller from Maharashtra to Karnataka.

2. Material and methods

2.1. Ethics statement

The study protocol was reviewed and approved by the NIMHANS Institutional Ethics Committee vide NIMHANS/IEC/2020–21.

2.2. Cells

The Vero E6 cell line (C1008) and Vero CCL-81 cells were grown and maintained in Dulbecco's Modified Eagle's Medium (DMEM) (Gibco, USA) supplemented with 10% heat-inactivated fetal bovine serum (FBS) (Gibco, USA), 100 U/ml Penicillin, 100 µg/ml Streptomycin (Gibco, USA) and 2.5 µg/ml Amphotericin B (Neon Lab, India) (complete medium).

2.3. Clinical specimen, virus isolation, propagation and plaque assay

Combined Nasopharyngeal swab (NS) and oropharyngeal swab (OS) specimens in Viral Transport Medium (VTM) received for SARS-CoV-2 testing at the Department of Neurovirology, NIMHANS were subjected to RNA extraction using QIAamp Viral RNA Mini Kit (Qiagen). Real-time PCR was performed using RealStar SARS-CoV-2 RT PCR Kit (Altona Diagnostic). Specimens positive for SARS-CoV-2 were subjected to Whole Genome Sequencing (WGS) and virus isolation in the BSL3 facility. Monolayer of Vero cells was inoculated with the specimens and incubated at 37 °C with 5% CO_2 for 1 h. Unabsorbed virus was discarded and the cells were incubated further for 96 h in complete medium. The supernatant from wells showing CPE was used to propagate the virus. For the growth curve, cells were infected with SARS-CoV-2 at MOI 1 and the supernatant was collected at 0 to 72 hpi and cryopreserved. Plaque assay was performed using the supernatant to quantify the viral titre at different timepoints.

2.4. Virus titration by plaque assay

The infection was carried out in Vero E6 cells as described above. Upon adsorption, the cells were overlaid with agarose and incubated at 37 °C with 5% CO_2 for 72 h. The cells were fixed with formal saline and stained with crystal violet. Plaques were counted and virus titre was calculated using the standard formula [12].

2.5. RNA extraction and PCR

The RNA was extracted using an RNA extraction kit (Chemagic Viral DNA/RNA Kit special H96) as per manufacturer's instructions. Real-time PCR was carried out using the COVIDsure Multiplex Real-time RT-PCR Kit (Trivitron Healthcare Pvt. Ltd.). The amplification and data analysis were performed in the QuantStudio 6 PCR machine (Thermofisher Scientific).

2.6. Immunofluorescence assay (IFA)

Smears of SARS-CoV-2 infected Vero cells were stained with monoclonal antibodies against SARS-CoV-2 spike protein (1c10.c2 and 2c3.h6, Syngene Int. Ltd.) and fluorescein (FITC) goat anti-mouse IgG (H + L) secondary antibody (Life Technologies). The slide was mounted and visualized under a fluorescent microscope (Life Technologies).

2.7. Electron Microscopy

Negative staining of SARS-CoV-2 virus particles: SARS-CoV-2 infected Vero cell culture supernatant was fixed with 2% aqueous glutaraldehyde, dropped on collodion-coated copper grids and stained with 2% aqueous uranyl acetate (TAAB Lab, UK). The grids were visualized by transmission electron microscopy (TEM) (JEM-1400 Plus, Japan).

Staining of SARS-CoV-2 infected Vero cell monolayer: SARS-CoV-2 infected Vero cells were fixed at 36 hpi with 2.5% buffered glutaraldehyde and post-fixed with 1% buffered osmium tetroxide (TAAB, UK). Dehydration was performed using graded series of alcohol (70%, 80%, 90%, and 100%) and cleared using propylene oxide (Sigma, USA). The released monolayer was embedded in CY212 araldite resin (TAAB, UK) and polymerized. Ultrathin sections (60–70 nm) were collected on copper grids and contrasted using saturated methanolic uranyl acetate and 0.2% lead citrate. Stained sections were visualized under TEM.

2.8. Whole Genome Sequencing (WGS)

The amplicon sequencing approach was used for WGS as described by ARTIC Network protocol [13]. The V3 primer set has 109 pairs with amplicons of about 400 base pairs (bp) covering the whole genome except 31 bp of 5′ and a part of the 3' UTR region. Adjacent/overlapping primers were pooled into different pools to prevent preferential amplification of short fragments between adjacent primer pairs and PCR was performed. The barcoding of the resulting amplicons was done using the native barcoding (NBD 104/114) approach combined with the ligation sequencing kit (SQK-LSK109) and the libraries for Nanopore sequencing was prepared. The resulting DNA was cleaned and sequenced using MinION with the FLO-MIN-106 flow cell.

2.9. Analysis of sequence data

Sequencing data analysis was performed as described previously [14]. Briefly, sequences obtained were base called and demultiplexed using guppy (v5.0.11). Reads between 100 bp and 600 bp were taken up for further analysis. Amplicon sequencing primers were removed by trimming 25 bp at the ends and additional trimming based on alignment using BBduk (v38.37). Minimap2 (v2.17) within Geneious Prime (Geneious Prime 2020.0.3) was used to map the resulting reads using the RefSeq strain (NC_045512.2). A consensus genome was generated with >10× coverage and a 0% majority rule. The resulting consensus genome was then aligned to the reference genome to ensure the correct reading frame and annotation were transferred from the reference sequence.

Eighty-five genome sequences of SARS-CoV-2 were used for phylogenetic tree analysis with reference sequence NC_045,512 as an outgroup. MUSCLE was used for multiple sequence alignment and iqtree (v1.6.12) was used to infer the phylogeny [15,16]. The substitution model for the phylogeny analysis used was GTR+F+I, and the sequences were downloaded from Global Initiative on Sharing All Influenza Data (GISAID) database [17]. The Pangolin assignment was assigned using the online tool (Pangolin COVID-19 lineage assigner version v3.1.14).

Mutations were checked using the online tool Nextclade and compared with the reference sequence (NC_045512.2). The mutations in the sequences from the clinical specimen and the isolate were compared. Further, analysis of the total 979 complete sequences of SARS-CoV-2 available on GISAID database from Maharashtra and Karnataka during the period January–June 2020 was performed to determine the prevalence of different lineages. Phylogenetic analysis was performed to assess linkage between different lineages using at least one sequence from each pango lineage available during the period from Maharashtra.

2.10. Statistical analysis

The results are represented as mean ± standard error mean. GraphPad PRISM (v9.0.1) and Microsoft Excel (v16.16.27) was used for data analysis.

3. Results

3.1. Clinical specimen, virus isolation and plaque assay

The combined NS and OS specimen from a 50-year-old male asymptomatic traveller from Maharashtra to Karnataka that tested positive in May 2020 for SARS-CoV-2 by RT PCR was subjected to WGS and SARS-CoV-2 isolation. Vero cells inoculated with the specimen showed typical CPE such as rounding and detachment following 96 hpi. The virus isolation was confirmed by Real-time RT-PCR and was propagated by passaging in Vero E6 cells. Plaque assay was performed to quantify the virus. The highest viral titre obtained with Vero cell CCL81 was 2.5 × 104 pfu/ml while the titre was 5 × 106 pfu/ml in Vero E6. The plaques formed in infected Vero E6 monolayer are depicted in Fig. 1.

3.2. Immunofluorescence, bright-field microscopy and growth curve

The mock-infected Vero cells showed negligible background fluorescence (Fig. 2, Panel A) as compared to infected Vero cells that showed extensive fluorescence, confirming infection with SARS-CoV-2 virus (Fig. 2, Panel B), upon staining with anti-spike monoclonal antibodies.

SARS-CoV-2 infection at MOI 1 in Vero E6 cells showed typical cytopathic effect such as rounding, granulation and detachment as early as 12 hpi. However, at 36 h and 48 h post-infection, most cells were found detached from the plate (Fig. 3a). Growth kinetics by plaque assay of the culture supernatant revealed highest viral titre at 24 hpi (Fig. 3b).

3.3. Transmission Electron Microscopy

Negative staining of the isolated SARS-CoV-2 virus particles showed typical crown appearance with the spikes on the surface and inner electron-dense granular region corresponding to the nucleocapsid material thereby establishing the isolation of the virus. The diameter of the virus particle, with spikes, ranged between ~70 and 90 nm (Fig. 4a).

TEM studies at 36 hpi showed that the mock-infected Vero cells were spindle-shaped and elongated. The cytoarchitecture of the cells revealed abundant cytoplasm with the normal distribution of cytoplasmic organelles. Elliptical nuclei (N) were seen in the centre of cells. Numerous mitochondria with normal cristae pattern, rough endoplasmic reticulum (RER), golgi apparatus (GA), small vacuoles and polyribosomes were well appreciated (Fig. 4c). There were no abnormalities in the sub-cellular structures.

Distinct ultrastructural changes were noted in SARS-CoV-2 infected cells with virions adhered to the cell membrane (Fig. 4d and e). Some cells appeared bloated due to the accumulation of several membrane-bound vesicles containing pleomorphic virions in the cytoplasm. The diameter of the SARS-Cov-2 virions ranged ~70 nm to 90 nm (Fig. 4h and i). The infected cells displayed a spherical eccentric nucleus, normal nuclear membrane, and no overt chromatin changes. A few infected cells showed apoptotic changes such as electron-dense cytoplasm with fragmented nucleus lacking distinct nuclear membrane (Fig. 4j and k).

Additionally, distinct single or multiple intranuclear ~8–10 nm filamentous inclusions were observed in a few infected cells (Fig. 4l). Numerous membrane-bound vesicles were also seen with granular content of varying electron density within the cytoplasm of apoptotic cells (Fig. 4k). RER and GA appeared to be dilated. One focus of dilated RER with viral particles was evident in an infected cell (Supplementary Fig. 1a). The size of the mitochondria in infected cells varied with loss of cristae pattern compared to 36 h mock-infected cells (Supplementary Fig. 1c).

3.4. Whole Genome Sequencing (WGS)

The WGS of the clinical specimen revealed 12 nucleotide mutations, resulting in six amino acid mutations. The 12 nucleotide mutations were C241T, C1684T, G2819T, C3037T, C3634T, T4949C, C8025T, C14408T, C15324T, A23403G, G28899T, and C29376T. The six amino acid substitutions, includes D614G in S gene, V852L, A2587V in ORF1a gene, P314L in ORF1b gene, and R209I, P368L in N gene as depicted in Supplementary Table 3. The clinical specimen sequence is uploaded to the GISAID database with GISAID epi id EPI_ISL_515,968 and identified as lineage B.1.210 using Pangolin COVID-19 lineage assigner. Further, the sequence of the viral isolate had one additional nucleotide mutation at T26327C, resulting in L28P amino acid substitution in the E gene, acquired during passaging of the virus. The sequence is uploaded to the GISAID database with GISAID epi id EPI_ISL_8740588 and was identified as the pangolin lineage B.1.210 similar to that of the clinical specimen.

3.5. Sequence and phylogenetic analysis

The phylogenetic tree (Fig. 5) was constructed using sequences downloaded from GISAID (Supplementary Table 1), and the sequences of the clinical specimen and viral isolate showed 100% similarity. Additionally, it was found that the isolated virus of lineage B.1.210 is closely related to the original Wuhan virus reference sequence and clustered with other sequences of the same lineage.

Among the 979 complete SARS-CoV-2 sequences uploaded from Maharashtra and Karnataka during January–June 2020, B.1.210 lineage was second and fourth most prevalent lineage in Maharashtra and Karnataka respectively (Supplementary Tables 4a and b) [18]. Further, phylogenetic analysis among sequences of each lineage from Maharashtra during this period revealed linkage between B.1.210 with other

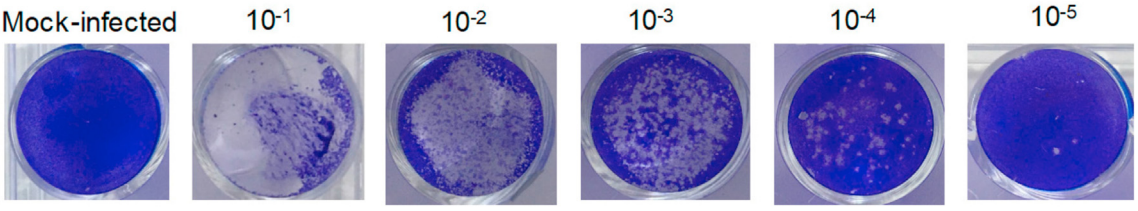

Fig. 1. SARS-CoV-2 plaque assay with Vero E6 monolayer showing reduction in number of plaques at higher dilutions of the virus culture at 72 h post infection when stained with crystal violet after fixing with formal saline.

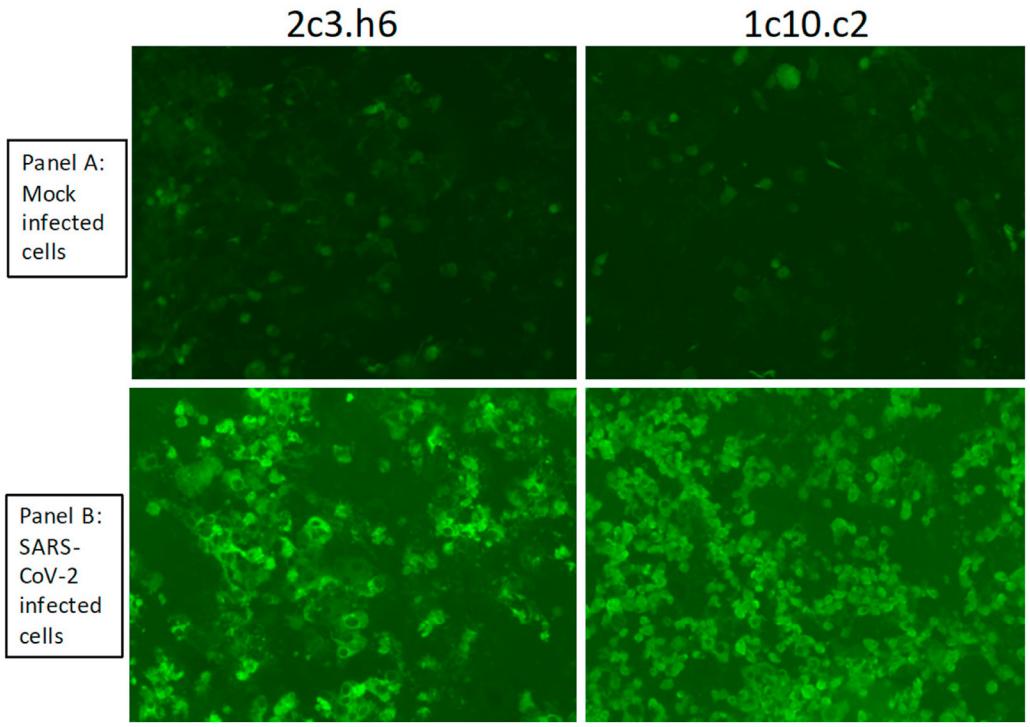

Fig. 2. Immunofluorescence assay to identify SARS-CoV-2 showing prominent apple-green fluorescence in infected Vero cells as compared to mock-infected cells after staining with monoclonal antibodies against spike protein of SARS-CoV-2.

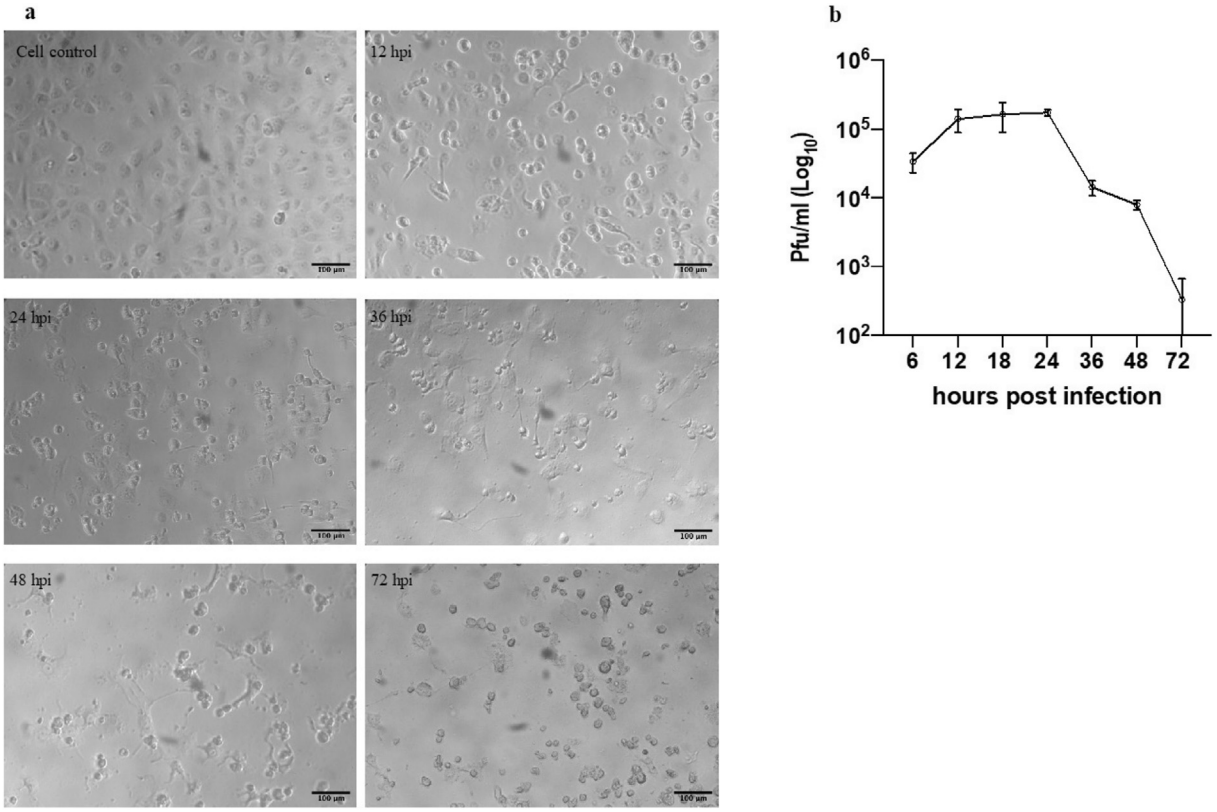

Fig. 3. (A) Bright field microscopy of SARS-CoV-2 infected Vero E6 cells showing CPE such as rounding and detachment at different timepoints post infection as compared to mock-infected cell control (b) Growth kinetics of SARS-CoV-2 in infected Vero E6 cells showing highest viral titre at 24 h post infection.

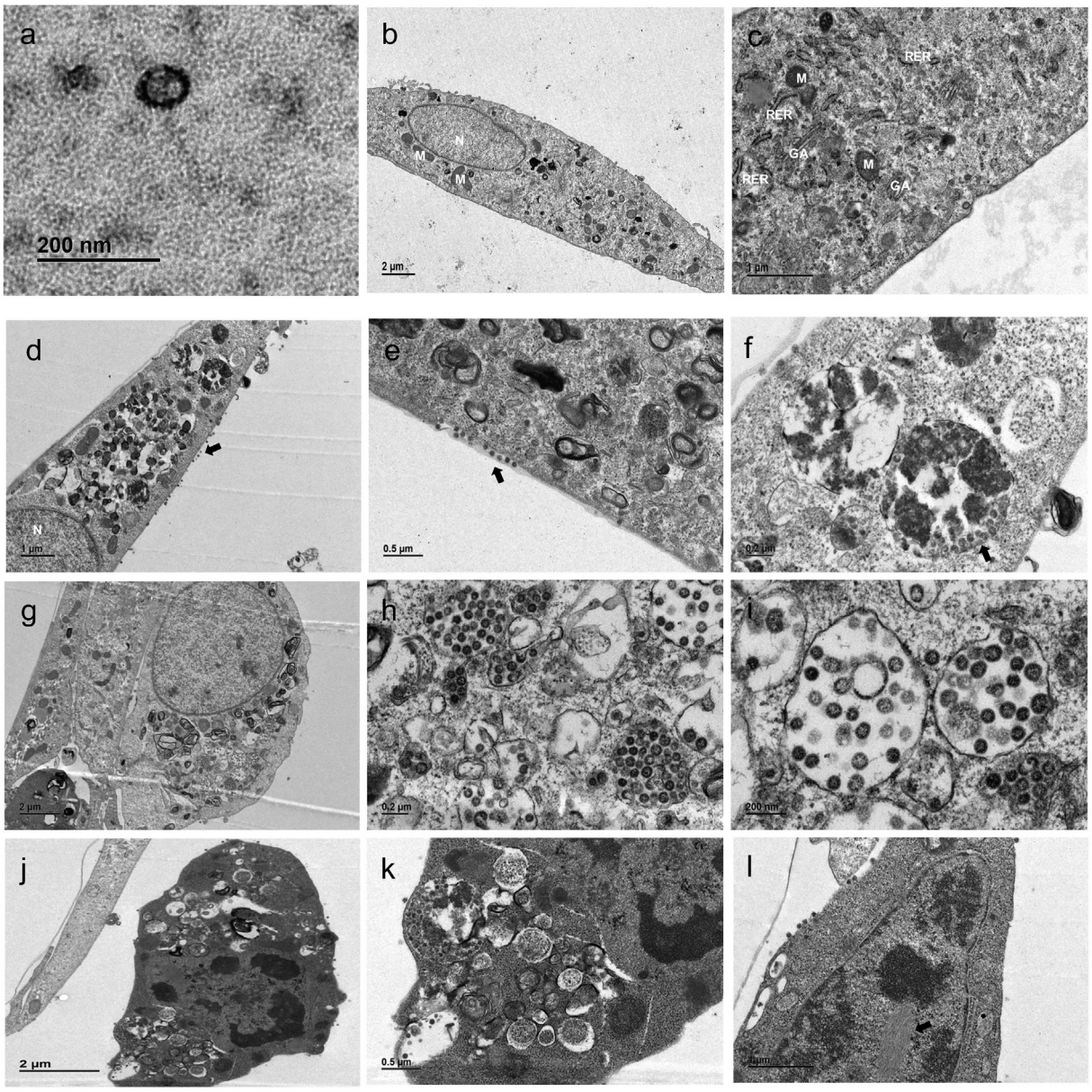

Fig. 4. Transmission Electron Microscopy (a) Negative staining of SARS-CoV-2 viral particle (b) mock-infected Vero cell at low magnification showing spindle-shaped, elongated cell with prominent nucleus (N) and mitochondria (M), x1200 (c) High magnification of cytoplasmic contents of mock-infected Vero cell with typical subcellular structures [mitochondria (M), rough endoplasmic reticulum (RER), golgi apparatus (GA)], x5000 (d) low magnification showing spindle-shaped cell with numerous viral particles adsorbed onto the cell surface (arrow), cytoplasm filled with multiple single membrane bound structures containing membranous whorls with varying electron density and a portion of the nucleus (N), x2500 (e) High magnification showing viral particles adhered at the cell surface (arrow) and cytoplasm containing membranous whorls resembling myelinic figures, x6000 (f) High magnification of membrane-bound vesicles with numerous nascent virions (arrow) and granular material, x10000 (g) Low magnification of a swollen infected Vero cell with eccentric nucleus, multiple membrane-bound vesicles with viral particles, and membranous structures in the cytoplasm, x1500 (h) Numerous virions of varying size encapsulated within the membrane-bound structures, x10000 (i) Higher magnification of membrane-bound vesicles with several pleomorphic virions of varying electron density, x15000 (j) Low magnification of infected cell with fragmented nucleus, electron-dense cytoplasm containing numerous membrane-bound structures consisting of virions along with granular structures, x2000 (k) High magnification of multiple membrane-bound structures containing virions with granular material, x6000 (l) Infected Vero cell with viral particles adhered to the cell surface and intranuclear filamentous inclusions (arrow), x5000.

strains which similarly evolved from parent lineage B during the first wave of pandemic (Supplementary Fig. 2).

4. Discussion

SARS-CoV-2 virus isolated from a traveller to Karnataka state from Maharashtra showed features of pathogenesis in Vero cells as reported earlier [19]. The Vero E6 cell line supported higher infection and amplification of SARS-CoV-2 as compared to Vero-CCL81, similar to previous studies [19]. Ultrastructural studies by TEM showed the characteristic morphology of isolated SARS-CoV-2 virus particle which is spherical in shape with spikes on the surface, measuring 70–90 nm [2]. At 36 hpi, we observed membrane-bound vacuoles, either empty or loaded, with immature virions and a few double-membrane vesicles, similar to a previous study [20]. Infected cells also showed distinct single/multiple intranuclear filamentous inclusions in the nucleoplasm similar to that reported in H1N1 infected human skeletal muscle cells [21]. Infected cells revealed the presence of virions at the cell surface, suggesting release of

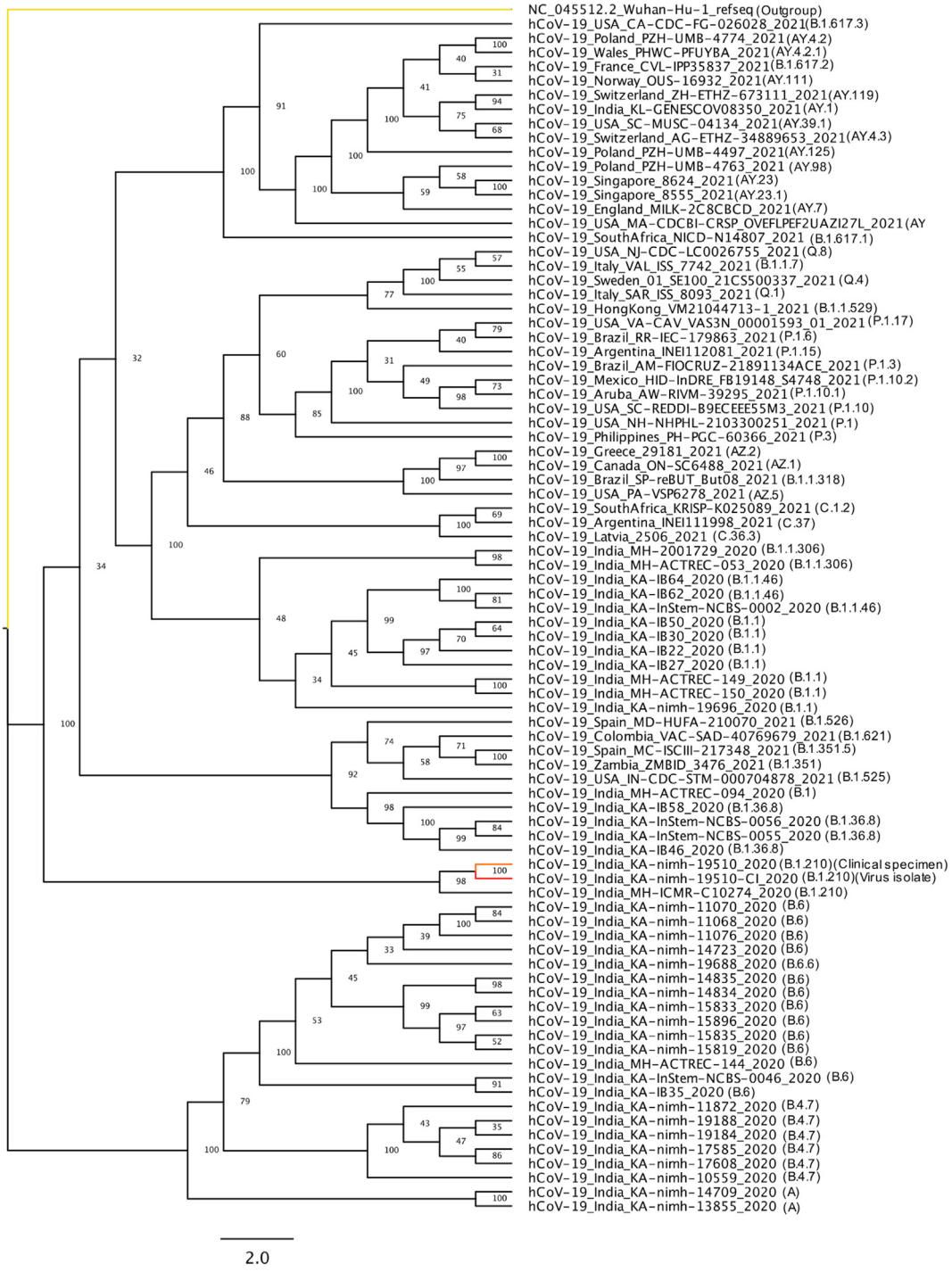

Fig. 5. Maximum likelihood phylogenetic tree was constructed using a total of 85 sequences which included 83 sequences downloaded from GISAID database and the sequences from clinical specimen and the viral isolate, along with NC_045512.2 reference sequence as outgroup. The sequence from clinical specimen (pink) and the viral isolate (red) are closely related to the original Wuhan strain and other strains of lineage B. The numbers at each node represent bootstrap value (in %).

viral particles by exocytosis. Mitochondria of varying sizes were observed with loss in the cristae pattern as reported earlier [22]. The absence of normal RER and GA with the presence of viral particles in the lumen of dilated RER and within membrane-bound vesicles strongly suggest that these subcellular structures transform into virus replicating factories [20]. The presence of numerous myelin-like structures in the cytoplasm of infected cells clearly indicates the accumulation of degraded products, possibly due to the autophagic process. Unlike a previous report, we did not observe the presence of lipid droplets in Vero cells at 36 hpi [22]. TEM of an infected cell revealed probable endocytosis of virus particles, with the cell membrane appearing intact and forming an endocytic vesicle-like structure (Supplementary Fig. 1b).

The whole genome sequences, of the clinical specimen and the virus isolate, belonged to the Pangolin lineage B.1.210, which was widely circulating in India during the early phase of the first wave in 2020. A total of 465 sequences have been reported globally of this lineage until January 15, 2022, out of which India has reported 370 (80%) sequences (Supplementary Table 2). The first sequence reported is from Maharashtra, detected on March 10, 2020, suggesting the origin and spread of this particular lineage in India.

The significant spike protein mutation in this lineage reported is D614G, which is suggested to render the virus more infectious [23,24]. The phylogenetic tree analysis also showed clustering of sequences from the clinical specimen and the virus isolate with the B.1.210 lineage sequence. In fact, lineage B.1.210 was the second most prevalent variant during January–June 2020 in Maharashtra showing linkage with other strains of SARS-CoV-2 that evolved from the parent lineage B.

During the first wave of the pandemic in India, Maharashtra was the worst-hit state [25]. Consequent to the revised travel guidelines during the lockdown by the Karnataka government, allowing a one-time movement of people from the state stranded elsewhere on May 4, 2020, there was a massive influx of people from Maharashtra and other states resulting in a sudden surge of cases in Karnataka in the following weeks [26]. The SARS-CoV-2 virus of the lineage B.1.210 reported here, was in fact, isolated from the clinical specimen of one such asymptomatic traveller from Maharashtra.

5. Conclusion

The SARS-CoV-2 variant B.1.210 virus isolated here showed ultrastructural features and cytopathogenesis similar to that of the virus reported during early phase of pandemic. Genomic characterization revealed the D614G mutation that is implicated in enhanced infectivity. Phylogenetic analysis showed that the whole genome sequence of the isolated virus is closely related to the original Wuhan virus reference sequence, thereby suggesting that the SARS-CoV-2 lineage B.1.210 that was circulating in India during the early phase of pandemic is likely to have evolved from the original Wuhan strain.

Author contribution

NK wrote the protocol, performed experiments, analyzed data, prepared and reviewed the manuscript. RK contributed to TEM studies. JA and SJ contributed to IFA experiments. PP and AKG contributed WGS. GN contributed to planning and review of TEM studies. AD, VR contributed to planning of the study and reviewed the manuscript. MMV designed the study, wrote the protocol, supervised the experiments, prepared and reviewed the manuscript.

Conflict of interest

The authors declare no conflict of interest.

Funding

The study was supported by core funds of the Department of Neurovirology, NIMHANS.

Acknowledgements

The authors would like to thank the healthcare facilities that availed the COVID-19 RT PCR services at NIMHANS. We are thankful to Dr. Bhupesh Mehta, Department of Biophysics, NIMHANS for his support with microscopy equipment. We thank all the members of the COVID-19 RT PCR lab at NIMHANS and the staff of the Electron Microscopy facility. We would like to thank Dr. Chitra Pattabiraman for her support with WGS.

Appendix A. Supplementary data

Supplementary data to this article can be found online at https://doi.org/10.1016/j.ijmmb.2022.12.009.

References

[1] Su S, Wong G, Shi W, Liu J, Lai ACK, Zhou J, et al. Epidemiology, genetic recombination, and pathogenesis of coronaviruses. Trends Microbiol 2016;24:490–502. https://doi.org/10.1016/j.tim.2016.03.003.
[2] Zhu N, Zhang D, Wang W, Li X, Yang B, Song J, et al. Brief report: a novel coronavirus from patients with pneumonia in China, 2019. N Engl J Med 2020;382:727. https://doi.org/10.1056/NEJMoa2001017.
[3] Zhou P, Yang X-L, Wang X-G, Hu B, Zhang L, Zhang W, et al. A pneumonia outbreak associated with a new coronavirus of probable bat origin. Nature 2020;579:270–3. https://doi.org/10.1038/s41586-020-2012-7.
[4] Benvenuto D, Giovanetti M, Ciccozzi A, Spoto S, Angeletti S, Ciccozzi M. The 2019-new coronavirus epidemic: evidence for virus evolution. J Med Virol 2020;92:455–9. https://doi.org/10.1002/jmv.25688.
[5] Naming the coronavirus disease (Covid-19) and the virus that causes it n.d. https://www.who.int/emergencies/diseases/novel-coronavirus-2019/technical-guidance/naming-the-coronavirus-disease-(covid-2019)-and-the-virus-that-causes-it (accessed September 28, 2021).
[6] WHO Director-General's opening remarks at the media briefing on Covid-19-11 March 2020 n.d. https://www.who.int/director-general/speeches/detail/who-director-general-s-opening-remarks-at-the-media-briefing-on-covid-19–-11-march-2020 (accessed September 28, 2021).
[7] Bhosale S, Kulkarni AP. Is A problem shared, A problem halved? Not always! The novel coronavirus COVID-19 outbreak. Indian J Crit Care Med Peer-Rev Off Publ Indian Soc Crit Care Med 2020;24:88–9. https://doi.org/10.5005/jp-journals-10071-23365.
[8] Kumar N, Hameed SKS, Babu GR, Venkataswamy MM, Dinesh P, Kumar BGP, et al. Descriptive epidemiology of SARS-CoV-2 infection in Karnataka state, South India: transmission dynamics of symptomatic vs. asymptomatic infections. EClinicalMedicine 2021;32. https://doi.org/10.1016/j.eclinm.2020.100717.
[9] Pattabiraman C, Habib F, P K H, Rasheed R, Prasad P, Reddy V, et al. Genomic epidemiology reveals multiple introductions and spread of SARS-CoV-2 in the Indian state of Karnataka. PLoS One 2020;15:e0243412. https://doi.org/10.1371/journal.pone.0243412.
[10] Srivastava S, Banu S, Singh P, Sowpati DT, Mishra RK. SARS-CoV-2 genomics: an Indian perspective on sequencing viral variants. J Biosci 2021;22:46. https://doi.org/10.1007/s12038-021-00145-7.
[11] Stelzer-Braid S, Walker GJ, Aggarwal A, Isaacs SR, Yeang M, Naing Z, et al. Virus isolation of severe acute respiratory syndrome coronavirus 2 (SARS-CoV-2) for diagnostic and research purposes. Pathology 2020;52:760–3. https://doi.org/10.1016/j.pathol.2020.09.012.
[12] Baer A, Kehn-Hall K. Viral concentration determination through plaque assays: Using traditional and novel overlay systems. J Vis Exp JoVE 2014;52065. https://doi.org/10.3791/52065.
[13] Quick J. nCoV-2019 sequencing protocol v3 (LoCost). ProtocolsIo 2020. https://www.protocols.io/view/ncov-2019-sequencing-protocol-v3-locost-bh42j8ye. [Accessed 9 October 2021].
[14] Pattabiraman C, Prasad P, George AK, Sreenivas D, Rasheed R, Reddy NVK, et al. Importation, circulation, and emergence of variants of SARS-CoV-2 in the South Indian state of Karnataka. https://doi.org/10.12688/wellcomeopenres.16768.1; 2021.
[15] Nguyen L-T, Schmidt HA, von Haeseler A, Minh BQ. IQ-TREE: a fast and effective stochastic algorithm for estimating maximum-likelihood phylogenies. Mol Biol Evol 2015;32:268–74. https://doi.org/10.1093/molbev/msu300.
[16] Hoang DT, Chernomor O, von Haeseler A, Minh BQ, Vinh LS. UFBoot2: improving the ultrafast bootstrap approximation. Mol Biol Evol 2018;35:518–22. https://doi.org/10.1093/molbev/msx281.
[17] Shu Y, McCauley J. GISAID: Global initiative on sharing all influenza data - from vision to reality. Euro Surveill Bull Eur Sur Mal Transm Eur Commun Dis Bull 2017;22:30494. https://doi.org/10.2807/1560-7917.ES.2017.22.13.30494.
[18] database G. EPI_SET_221102zx. 2022.
[19] Harcourt J, Tamin A, Lu X, Kamili S, Sakthivel SK, Murray J, et al. Severe acute respiratory syndrome coronavirus 2 from patient with coronavirus disease, United States. Emerg Infect Dis 2020;26:1266–73. https://doi.org/10.3201/eid2606.200516.
[20] Eymieux S, Rouillé Y, Terrier O, Seron K, Blanchard E, Rosa-Calatrava M, et al. Ultrastructural modifications induced by SARS-CoV-2 in Vero cells: a kinetic analysis of viral factory formation, viral particle morphogenesis and virion release. Cell Mol Life Sci CMLS 2021;78:3565–76. https://doi.org/10.1007/s00018-020-03745-y.
[21] Desdouits M, Munier S, Prevost M-C, Jeannin P, Butler-Browne G, Ozden S, et al. Productive infection of human skeletal muscle cells by pandemic and seasonal influenza A(H1N1) viruses. PLoS One 2013;8. https://doi.org/10.1371/journal.pone.0079628.
[22] Nardacci R, Colavita F, Castilletti C, Lapa D, Matusali G, Meschi S, et al. Evidences for lipid involvement in SARS-CoV-2 cytopathogenesis. Cell Death Dis 2021;263:12. https://doi.org/10.1038/s41419-021-03527-9.
[23] Zhang L, Jackson CB, Mou H, Ojha A, Rangarajan ES, Izard T, et al. The D614G mutation in the SARS-CoV-2 spike protein reduces S1 shedding and increases infectivity. BioRxiv 2020. https://doi.org/10.1101/2020.06.12.148726. 2020.06.12.148726.

[24] Hasan MM, Das R, Rasheduzzaman M, Hussain MH, Muzahid NH, Salauddin A, et al. Global and local mutations in Bangladeshi SARS-CoV-2 genomes. Virus Res 2021;198390:297. https://doi.org/10.1016/j.virusres.2021.198390.
[25] India's first Covid-19 wave finally recedes. Hindustan Times; 2020. https://www.hindustantimes.com/india-news/india-s-first-covid-19-wave-finally-recedes/story-clQaMmmD2TiYD3i1CSmw3J.html (accessed December 22, 2021).
[26] Karnataka government to allow all industries to open from May 4 except in red zones- The New Indian Express n.d. https://www.newindianexpress.com/states/karnataka/2020/apr/30/karnataka-government-to-allow-all-industries-to-open-from-may-4-except-in-red-zones-2137467.html (accessed December 22, 2021).